


Statistical Mechanics of Directed Networks

Marián Boguñá ^{1,2,*} and M. Ángeles Serrano ^{1,2,3,*} 

¹ Department of Condensed Matter Physics, University of Barcelona, Martí i Franquès 1, E-08028 Barcelona, Spain

² University of Barcelona Institute of Complex Systems (UBICS), E-08028 Barcelona, Spain

³ Institució Catalana de Recerca i Estudis Avançats (ICREA), Passeig Lluís Companys 23, E-08010 Barcelona, Spain

* Correspondence: marian.boguena@ub.edu (M.B.); marian.serrano@ub.edu (M.Á.S.)

Abstract: Directed networks are essential for representing complex systems, capturing the asymmetry of interactions in fields such as neuroscience, transportation, and social networks. Directionality reveals how influence, information, or resources flow within a network, fundamentally shaping the behavior of dynamical processes and distinguishing directed networks from their undirected counterparts. Robust null models are crucial for identifying meaningful patterns in these representations, yet designing models that preserve key features remains a significant challenge. One such critical feature is reciprocity, which reflects the balance of bidirectional interactions in directed networks and provides insights into the underlying structural and dynamical principles that shape their connectivity. This paper introduces a statistical mechanics framework for directed networks, modeling them as ensembles of interacting fermions. By controlling the reciprocity and other network properties, our formalism offers a principled approach to analyzing directed network structures and dynamics, introducing new perspectives and models and analytical tools for empirical studies.

Keywords: complex networks; directed networks; maximum entropy; Fermi statistics; reciprocity



Academic Editors: Antonio M. Scarfone and Sergio Luiz E. F. Da Silva

Received: 19 December 2024

Revised: 9 January 2025

Accepted: 10 January 2025

Published: 18 January 2025

Citation: Boguñá, M.; Serrano, M.Á. Statistical Mechanics of Directed Networks. *Entropy* **2025**, *27*, 86. <https://doi.org/10.3390/e27010086>

Copyright: © 2025 by the authors. Licensee MDPI, Basel, Switzerland. This article is an open access article distributed under the terms and conditions of the Creative Commons Attribution (CC BY) license (<https://creativecommons.org/licenses/by/4.0/>).

1. Introduction

A directed network [1] is a representation of a complex system that captures the asymmetry of interactions between its elements [2,3]. Directionality enriches network structure [4,5], and is essential for understanding how influence, information, or resources flow through a system [6], fundamentally distinguishing directed networks from undirected ones. This is critical across a wide range of domains, including neuronal systems, biological processes, transportation systems, and social networks. Moreover, directionality fundamentally influences the behavior of dynamical processes on networks [7–10].

To gain a deeper understanding of the principles shaping real directed networks, it is crucial to define models that accurately capture their essential characteristics and organization. In general, network models enable researchers to distinguish meaningful patterns from random fluctuations and provide principled explanations for the observed regularities. The family of network models derived by maximizing the entropy of graph ensembles subject to the constraints imposed by observations in real-world networks offer the least biased prediction for their properties [11,12]. However, designing maximum entropy models for directed networks is a challenging task. This difficulty arises from the need to account for the interplay between local node properties and global network structures.

Specifically, key features in directed networks are in-degrees and out-degrees, accounting for the number of incoming and outgoing connected neighbors, their correlations, and reciprocity [11,13], or the tendency of pairs of nodes to form bidirectional connections. Reciprocity reflects the balance or imbalance of mutual interactions and serves as a critical indicator of the underlying structural and dynamical rules governing the system. Another key property is clustering, the tendency of pairs of neighbors to be connected, forming triangles in the network topology. In directed networks, triangles become multifaceted, splitting into seven distinct triangle motifs depending on the orientation of the arrows [14,15]. Despite the recent introduction of a directed network model [16] that simultaneously explains many features in directed networks, such as reciprocity, clustering, and other structural properties, a general theoretical approach based on the maximum entropy principle is still lacking.

In this paper, we introduce a statistical mechanics framework for directed networks, treating them as systems of interacting fermions. This approach leverages concepts from quantum statistics to describe directed networks in terms of ensembles, where network connections or fermions are constrained by conserved quantities and the entropy of the ensemble is maximized to fix its probability. By framing directed networks in this way, we provide a powerful theoretical tool for modeling their structure. Our framework not only offers new insights into the organization of real-world directed networks but also provides a principled basis for constructing models that respect key empirical properties.

2. General Formalism

The standard approach in network science treats the nodes of a network as the fundamental units of the system, with links representing the interactions between these units. This perspective naturally aligns with real-world systems, where nodes correspond to defined entities—countries in the world trade web, proteins or genes in biomolecular interaction networks, individuals in society, and so on—making focusing on nodes intuitive and practical. However, this node-centric viewpoint poses challenges when defining models using traditional tools from statistical mechanics, as it emphasizes the entities rather than the interactions.

In this work, we adopt a different perspective by shifting the focus from the nodes of the network to the links connecting them. In our approach, links are treated as fermionic “particles” that can occupy distinct energy states. The phase space of possible energy states is defined by the possible links between the N nodes of the network. This perspective is particularly intriguing for two reasons. First, links in a network are unlabeled, which makes them inherently indistinguishable. Second, in a simple network without multiple connections, only one link can occupy a given state, as no two identical links can exist between the same pair of nodes. These properties naturally lead to a statistical interpretation of links in a network as an ensemble of identical and independent fermions, obeying Fermi–Dirac statistics [11]. By reimagining directed networks in this manner, we not only provide a novel statistical framework for describing their structure but also lay the groundwork for constructing statistically rigorous principled models that capture the fundamental constraints of directed and undirected networks alike. For instance, fermionic mapping has been instrumental in the analytical study of different aspects of networks, from the explanation of structural correlations in scale-free networks [17] to a topological phase transition with divergent entropy involving the reorganization of network cycles [18].

2.1. Fermionic Approach to Directed Networks

Given a pair of nodes i and j , we define two distinct states, $i \rightarrow j$ and $j \rightarrow i$, which can be occupied by links, or fermions, pointing from i to j and from j to i , respectively,

see Figure 1. Each state $i \rightarrow j$ has an associated energy ϵ_{ij} . The occupancy of these states is described by the asymmetric adjacency matrix $\{a_{ij}\}$, which equals 1 if the state $i \rightarrow j$ is occupied and 0 otherwise, analogous to the occupation number of states in systems of indistinguishable particles. All the topological properties of the network can be computed from the adjacency matrix. For instance, the number of incoming connections to a node, or the incoming degree, is

$$k_{in,i} = \sum_{j=1}^N a_{ji},$$

where N is the total number of nodes in the network. Analogously, the number of outgoing connections from a node, or the outgoing degree, is

$$k_{out,i} = \sum_{j=1}^N a_{ij}.$$

Reciprocity implies pairs of nodes with links pointing in both directions, as shown in the sketch at the bottom of Figure 1. In random network models, a certain default level of reciprocity is attained when links are independent, or fermions are non-interacting. However, higher or lower values require that links are correlated, or fermions are interacting. To account for this possibility, we assume that the energy of two links occupying the two states $i \rightarrow j$ and $j \rightarrow i$ simultaneously, that is, of mutual interactions, is $\tilde{\epsilon}_{ij}$. In general, $\tilde{\epsilon}_{ij}$ is different from $\epsilon_{ij} + \epsilon_{ji}$.

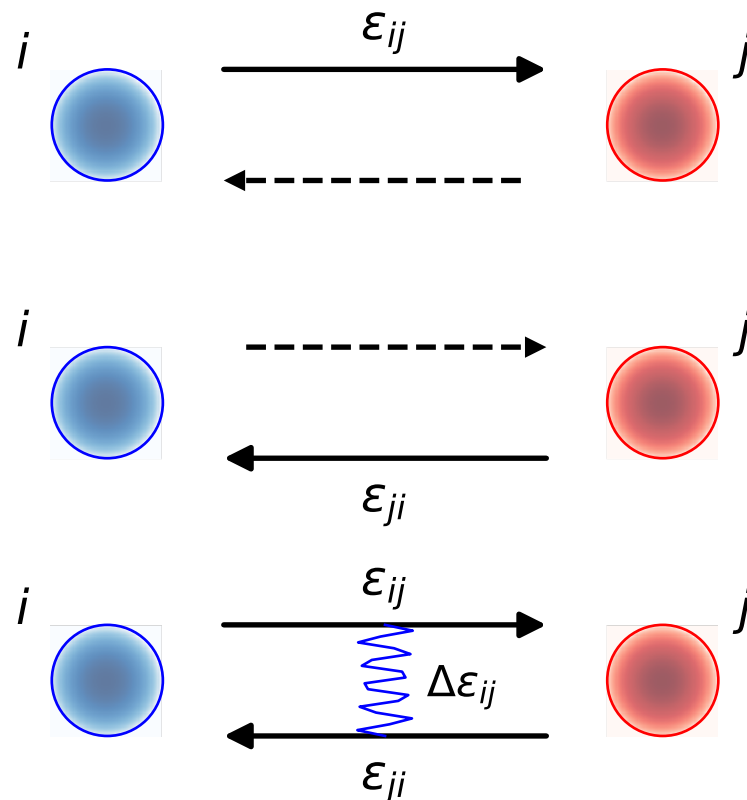


Figure 1. Possible fermionic states between a pair of nodes i and j , and their associated energies. The solid arrow indicates the presence of a directed link and the dashed arrow an empty state. When the two fermions simultaneously occupy the two states, $i \rightarrow j$ and $j \rightarrow i$, the total energy includes a correction $\Delta\epsilon_{ij}$ added to the sum of the energies of the partially occupied states.

Due to the indistinguishability of links in a network, any directed network can be represented in the Fock space using the basis $\{|a\rangle \equiv \otimes_{i,j} |a_{ij}\rangle\}$ defining the number of

particles/links occupying the set of possible single-particle states. Thus, the representation of the Hamiltonian of the network \hat{H} in the basis of the Fock space defined by the adjacency matrix is

$$\langle a | \hat{H} | a \rangle = \sum_{i < j} [a_{ij}\epsilon_{ij} + a_{ji}\epsilon_{ji} + a_{ij}a_{ji}\Delta\epsilon_{ij}], \tag{1}$$

where

$$\Delta\epsilon_{ij} = \tilde{\epsilon}_{ij} - \epsilon_{ij} - \epsilon_{ji}$$

is the correction due to the interaction of two fermions occupying the two states $i \rightarrow j$ and $j \rightarrow i$. When $\Delta\epsilon_{ij} > 0$, the presence of two links connecting the same pair of nodes in opposite directions is energetically unfavorable, and thus the reciprocity is lower than in the random case. Conversely, when $\Delta\epsilon_{ij} < 0$, the link reciprocity is higher than random case.

In analogy to the case of indistinguishable quantum particles, it is more convenient to work in the grand canonical ensemble, where the constraints are the following:

- the number of fermions (links) is fixed on average;
- The average energy is fixed as well.

In our formalism, this implies that the total number of links is a random variable that is fixed on average by the chemical potential μ . The grand partition function of the system is given by

$$\begin{aligned} Z &= \text{Tr} \left(e^{-\beta(\hat{H} - \mu\hat{N}_L)} \right) \\ &= \prod_{i < j} \left(1 + e^{-\beta(\epsilon_{ij} - \mu)} + e^{-\beta(\epsilon_{ji} - \mu)} + e^{-\beta(\tilde{\epsilon}_{ij} - 2\mu)} \right), \end{aligned} \tag{2}$$

where \hat{N}_L is the number of links operator and the inverse temperature β controls the average energy of the network. The chemical potential μ fixes the average in-degree (and out-degree) through the relation

$$\langle k_{\text{in}} \rangle = \langle k_{\text{out}} \rangle = \frac{1}{N\beta} \left(\frac{\partial \ln Z}{\partial \mu} \right)_{\beta}, \tag{3}$$

and the entropy of the ensemble can be computed from the partition function as

$$S = \ln Z - \beta \left(\frac{\partial \ln Z}{\partial \beta} \right)_{\mu}. \tag{4}$$

Beyond these global thermodynamic properties, the probability of the ensemble generating a graph with adjacency matrix $\{a_{ij}\}$ is computed as the probability of a particular configuration of the system

$$\text{Prob}(\{a_{ij}\}) = \frac{1}{Z} \prod_{i < j} e^{-\beta[(\epsilon_{ij} - \mu)a_{ij} + (\epsilon_{ji} - \mu)a_{ji} + a_{ij}a_{ji}\Delta\epsilon_{ij}]}. \tag{5}$$

The joint probability of the pair of states $i \rightarrow j$ and $i \leftarrow j$ between nodes i and j is

$$\text{Prob}(a_{ij}, a_{ji}) = \frac{e^{-\beta[(\epsilon_{ij} - \mu)a_{ij} + (\epsilon_{ji} - \mu)a_{ji} + a_{ij}a_{ji}\Delta\epsilon_{ij}]} }{1 + e^{-\beta(\epsilon_{ij} - \mu)} + e^{-\beta(\epsilon_{ji} - \mu)} + e^{-\beta(\tilde{\epsilon}_{ij} - 2\mu)}}. \tag{6}$$

Finally, the probability of a directed link existing between nodes i and j , $p_{ij} \equiv \text{Prob}(a_{ij} = 1)$, is

$$p_{ij} = \frac{e^{-\beta(\epsilon_{ij} - \mu)} + e^{-\beta(\tilde{\epsilon}_{ij} - 2\mu)}}{1 + e^{-\beta(\epsilon_{ij} - \mu)} + e^{-\beta(\epsilon_{ji} - \mu)} + e^{-\beta(\tilde{\epsilon}_{ij} - 2\mu)}}. \tag{7}$$

Equation (7) can be used to evaluate the average in- and out-degrees of individual nodes as

$$\kappa_{out,i} = \sum_j p_{ij}$$

and

$$\kappa_{in,i} = \sum_j p_{ji},$$

and the chemical potential as the solution of the equation

$$\langle \kappa_{in} \rangle N = \sum_{i,j,j \neq i} p_{ij}. \tag{8}$$

Finally, we can use these results to evaluate the reciprocity of the network r , defined as the ratio between the number of reciprocated links and the total number of links. Thus,

$$r = \frac{2 \sum_{i < j} p_{ij}(1,1)}{\sum_{i,j \neq i} p_{ij}}, \tag{9}$$

where we have defined $p_{ij}(1,1) \equiv \text{Prob}(a_{ij} = 1, a_{ji} = 1)$. It is important to mention here that the freedom to chose the interaction energies $\Delta\epsilon_{ij}$ enables the possibility to adjust the level of reciprocity for particular sets of nodes or with specific topological properties.

2.2. Non-Interacting Fermions

When the links are independent or, equivalently, the fermions are non-interacting, $\Delta\epsilon_{ij} = 0$ and the energy is $\tilde{\epsilon}_{ij} = \epsilon_{ij} + \epsilon_{ji}$. In this situation, the connection probability p_{ij} of a directed link between nodes i and j takes the simple form

$$p_{ij}^{ni} = \frac{1}{1 + e^{\beta(\epsilon_{ij} - \mu)}}. \tag{10}$$

The joint probability $\text{Prob}(a_{ij}, a_{ji})$ factorizes as $\text{Prob}(a_{ij}, a_{ji}) = p_{ij}^{ni} p_{ji}^{ni}$, and so does the partition function

$$Z = \prod_{i < j} \left(1 + e^{-\beta(\epsilon_{ij} - \mu)}\right) \left(1 + e^{-\beta(\epsilon_{ji} - \mu)}\right). \tag{11}$$

Finally, the reciprocity becomes

$$r = \frac{2 \sum_{i < j} p_{ij}^{ni} p_{ji}^{ni}}{\sum_{i,j \neq i} p_{ij}^{ni}}, \tag{12}$$

which corresponds to the reciprocity expected by pure chance.

2.3. Interacting Fermions

The connection probability of the system without interactions, p_{ij}^{ni} in Equation (10), can be used to rewrite the connection probability for a directed link in the case of interacting fermions, p_{ij} in Equation (7), which leads to

$$p_{ij} = p_{ij}^{ni} \frac{1 - p_{ji}^{ni} (1 - e^{-\beta\Delta\epsilon_{ij}})}{1 - p_{ij}^{ni} p_{ji}^{ni} (1 - e^{-\beta\Delta\epsilon_{ij}})}. \tag{13}$$

In the case of weak interactions or high temperature, the term $\beta\Delta\epsilon$ is small, leading to $p_{ij} \approx p_{ij}^{ni}$. Similarly, as seen from Equation (13), the connection probability remains unchanged by fermionic interactions in the limits $p_{ij}^{ni} \rightarrow 0$ or $p_{ij}^{ni} \rightarrow 1$, where $p_{ij} = p_{ij}^{ni}$ again

holds. In these extreme situations, the lack or excess of bidirectional links leaves no room for the network to exhibit sensitivity to changes in the tendency for reciprocity. We will use this general property in the next section when dealing with specific models.

3. Specific Random Network Models

So far, we have not specified the energies of the states $\{\varepsilon_{ij}\}$, which ultimately define the particular model at hand. To illustrate the power of our approach, we focus on two different models within our formalism: the non-interacting Directed Soft Configuration Model (NI-DCM) [11], and the non-interacting Directed Geometric Soft Configuration Model (NI-DGCM) [16]. Furthermore, we also derive their maximum entropy interacting counterparts (I-DCM and I-DGCM).

A priori, our formalism works for an arbitrary number of fermions between 0 and $N(N - 1)$. However, real complex networks are sparse, meaning that the average in- and out-degrees, $\langle k_{in} \rangle = \langle k_{out} \rangle$, are size-independent. In the rest of this paper, we consider ensembles of sparse networks.

3.1. Directed Configuration Model

To derive the probability of connection of the DCM [11,19] within our formalism, we make the simplest assumption that the energy of a directed link connecting nodes i and j comes from two sources: the energetic cost that node i incurs when creating an outgoing connection, $\varepsilon_{out,i}$, plus the energetic cost that node j incurs when accepting an incoming connection, $\varepsilon_{in,j}$. The total energy of the fermionic state is then

$$\varepsilon_{ij} = \varepsilon_{out,i} + \varepsilon_{in,j}. \tag{14}$$

Thus, each node in the network is characterized by an associated vector $(\varepsilon_{in}, \varepsilon_{out})$ accounting for incoming and outgoing connections. The distribution of such variables is given by the probability density function $\rho(\varepsilon_{in}, \varepsilon_{out})$, with marginal distributions for ε_{in} and ε_{out} , $\rho_{in}(\varepsilon_{in})$ and $\rho_{out}(\varepsilon_{out})$.

Although models in the DCM family are not fully realistic, they serve as prominent null models or baselines to evaluate whether observed features in real directed networks arise due to specific processes or simply by chance.

3.1.1. Non-Interacting Directed Configuration Model (NI-DCM)

Using Equation (8), and assuming that $\Delta\varepsilon_{ij} = 0$, and replacing sums with integrals, we can write

$$\langle k_{in} \rangle = Nz \int \int \frac{\rho_{in}(\varepsilon_{in})\rho_{out}(\varepsilon_{out})}{z + e^{\beta\varepsilon_{in}}e^{\beta\varepsilon_{out}}} d\varepsilon_{in}d\varepsilon_{out}, \tag{15}$$

where we have defined the fugacity in the standard way as $z \equiv e^{\beta\mu}$. Imposing sparsity in the thermodynamic limit of this particular model implies that the fugacity must scale with the system size as $z \sim N^{-1}$. This implies that the chemical potential takes the size-dependent form

$$\mu = \frac{1}{\beta} \ln \left[\frac{\langle k_{in} \rangle}{N \langle e^{-\beta\varepsilon_{in}} \rangle \langle e^{-\beta\varepsilon_{out}} \rangle} \right], \tag{16}$$

provided that $\langle e^{-\beta\varepsilon_{in}} \rangle$ and $\langle e^{-\beta\varepsilon_{out}} \rangle$ are bounded. In this case, the dependence between expected in- and out-degrees of nodes, κ_{in} and κ_{out} , and the in and out-energies, ε_{in} and ε_{out} , become

$$\kappa_{in} = \frac{\langle k_{in} \rangle}{\langle e^{-\beta\varepsilon_{in}} \rangle} e^{-\beta\varepsilon_{in}} \quad \text{and} \quad \kappa_{out} = \frac{\langle k_{out} \rangle}{\langle e^{-\beta\varepsilon_{out}} \rangle} e^{-\beta\varepsilon_{out}}. \tag{17}$$

Substituting Equation (14) into Equation (10) and using Equations (16) and (17), the connection probability in Equation (10) becomes the one for the directed soft configuration model:

$$p_{ij}^{ni} = \frac{1}{1 + \frac{\langle k_{in} \rangle N}{\kappa_{out,i} \kappa_{in,j}}} \tag{18}$$

Notice that, when the energies of states in Equation (14) are temperature-independent, the limit $\beta \rightarrow 0$ converges to the directed version of the classical Erdős-Rényi ensemble [20] because, in this limit, the expected degree of all nodes converges to the same value, as can be seen from Equation (17). In the opposite limit, when $\beta \gg 1$, the degree distribution becomes heavy-tailed and, depending on the distribution of energies, it may undergo a phase transition to a condensed phase where a finite fraction of nodes accumulate an extensive number of links, as shown in [21]. This effect will occur when the averages $\langle e^{-\beta \epsilon_{in}} \rangle$ and/or $\langle e^{-\beta \epsilon_{out}} \rangle$ diverge for $\beta > \beta_c$ for a critical inverse temperature β_c .

An alternative approach to Equation (14) is to fix the expected in- and out-degree distributions by defining temperature-dependent energy levels as

$$\epsilon_{ij} = -\frac{1}{\beta} \ln(\kappa_{out,i} \kappa_{in,j}), \tag{19}$$

and the chemical potential as

$$\mu = -\frac{1}{\beta} \ln[\langle k_{in} \rangle N]. \tag{20}$$

These choices lead to the same connection probability Equation (18), with the difference that now the expected in- and out-degrees are temperature-independent and, thus, the degree distribution is fixed. Temperature-dependent energy levels appear in strongly interacting systems [22–25].

The entropy of the ensemble can be calculated using Equation (4), whose leading terms are

$$S = \langle k_{in} \rangle N (\ln[\langle k_{in} \rangle N] - 1) + O(\ln N), \tag{21}$$

recovering results in [12]. Notice that this expression does not depend on the ensemble temperature, only on the total number of links, which is a property that is fixed in the ensemble and does not depend on the degree distribution. This means that the same expression holds in the alternative definition of the model where the energy of the states is temperature-dependent.

Finally, the reciprocity of the ensemble can be evaluated using Equation (12), and reads

$$r = \frac{\langle k_{in} k_{out} \rangle^2}{N \langle k_{in} \rangle^3} - \frac{\langle k_{in}^2 k_{out}^2 \rangle}{N^2 \langle k_{in} \rangle^3} \approx \frac{\langle k_{in} k_{out} \rangle^2}{N \langle k_{in} \rangle^3}. \tag{22}$$

Thus, the reciprocity of the NI-SCM vanishes in the thermodynamic limit, even though it can become significant if the in- and out-degrees of nodes are positively correlated and their distributions heavy-tailed.

3.1.2. Interacting Directed Configuration Model (I-DCM)

The probability for a directed link in this model can be found by substituting Equation (14) into Equation (7), with $\Delta \epsilon_{ij} \neq 0$, and imposing sparsity, which would again lead to Equations (16) and (17) if $\langle e^{-\beta \epsilon_{in}} \rangle$ and $\langle e^{-\beta \epsilon_{out}} \rangle$ are bounded. Alternatively, Equation (13), which relates the connection probabilities in the interacting and non-interacting formulations, provides a shortcut. The connection probability of the NI-DCM is size-dependent with p_{ij}^{ni} scaling as N^{-1} , hence approaching zero in the thermody-

dynamic limit. At this extreme, Equation (13) indicates that $p_{ij} \approx p_{ij}^n$, which implies that the energies ε_{in} and ε_{out} , along with β and μ , define the in- and out-degree distributions as in the non-interacting model.

In contrast, the joint probability $\text{Prob}(a_{ij}, a_{ji})$ in the I-DCM does not factorize, thereby enabling the tuning of the reciprocity. The reciprocity can be calculated from Equation (9), using the probability of having a bidirectional connection between nodes i and j from Equation (6) after imposing the condition that, the two links are present simultaneously, $a_{ij} = a_{ji} = 1$. Using that

$$e^{\beta(\varepsilon_{ij}-\mu)} = \frac{N\langle k_{in} \rangle}{\kappa_{out,i}\kappa_{in,j}},$$

the reciprocity is

$$r = \frac{2}{N\langle k_{in} \rangle} \times \sum_{i < j} \frac{\frac{\kappa_{out,i}\kappa_{in,j}}{N\langle k_{in} \rangle} \frac{\kappa_{out,j}\kappa_{in,i}}{N\langle k_{in} \rangle} e^{-\beta\Delta\varepsilon_{ij}}}{1 + \frac{\kappa_{out,i}\kappa_{in,j}}{N\langle k_{in} \rangle} + \frac{\kappa_{out,j}\kappa_{in,i}}{N\langle k_{in} \rangle} + \frac{\kappa_{out,i}\kappa_{in,j}\kappa_{out,j}\kappa_{in,i}}{N\langle k_{in} \rangle^2} e^{-\beta\Delta\varepsilon_{ij}}}, \tag{23}$$

which, up to leading order in N , gives

$$r = \frac{1}{(N\langle k_{in} \rangle)^3} \sum_{i,j} \kappa_{out,i}\kappa_{in,i}\kappa_{out,j}\kappa_{in,j} e^{-\beta\Delta\varepsilon_{ij}}. \tag{24}$$

This result implies that reciprocity vanishes in the thermodynamic limit. The specific form in which $r \rightarrow 0$ as $N \rightarrow \infty$ depends on the form of the interaction energy. In all cases, when $\Delta\varepsilon_{ij} > 0$, reciprocity is energetically unfavorable, and thus lower than in the NI-SCM for the same temperature; conversely, when $\Delta\varepsilon_{ij} < 0$, the link reciprocity is higher.

For instance, a constant value independent of the specific pair of nodes, $\Delta\varepsilon_{ij} = \varepsilon$, leads to

$$r = \frac{e^{-\beta\varepsilon}}{N\langle k_{in} \rangle^3} \langle k_{in}k_{out} \rangle^2, \tag{25}$$

meaning that the interaction introduces temperature-dependent rescaling as compared to the reciprocity of the NI-SCM in Equation (22).

If, instead of a constant value, the nodes in the interaction have an additive contribution to the interaction correction energy, $\Delta\varepsilon_{ij} = \varepsilon_i + \varepsilon_j$, then

$$r = \frac{1}{N\langle k_{in} \rangle^3} \left(\sum_i \kappa_{out,i}\kappa_{in,i} e^{-\beta\varepsilon_i} \right)^2. \tag{26}$$

If ε_i is proportional to the temperature, $\varepsilon_i \propto 1/\beta$, the NI-SCM behavior is recovered with a temperature-independent constant rescaling. Additionally, it can incorporate dependencies on the hidden degrees of the corresponding node, for instance, $\varepsilon_i = -1/\beta \ln(\kappa_{out,i}\kappa_{in,i})$, and then

$$r = \frac{1}{N\langle k_{in} \rangle^3} \langle (k_{in}k_{out})^2 \rangle. \tag{27}$$

Again, local correlations between the incoming and outgoing degrees of a node control the velocity of the reciprocity's decay. The results above also imply that a size-dependent negative interaction energy with intensity $|\varepsilon| \propto 1/\beta \ln N$ could counteract the decay of reciprocity in the SCM model and produce a finite value even in the thermodynamic limit.

3.2. Directed \mathbb{S}^d Model

As we have seen in the previous section, reciprocity vanishes in the thermodynamic limit of the DCM even when fermions interact. Similarly, clustering also vanishes due to the size dependence of the connection probability. Finite reciprocity and clustering can be achieved in the framework of geometric networks [26,27], where nodes are distributed in an underlying metric space such that a distance x_{ij} can be defined between any pair of nodes. In this situation, we assume that the energies of sending out or accepting a link are supplemented with a cost associated with the distance between the nodes. Thus, the total energy of a link is

$$\varepsilon_{ij} = \varepsilon_{out,i} + \varepsilon_{in,j} + f(x_{ij}), \tag{28}$$

where $f(x)$ is a monotonically increasing function of the distance. An interesting choice is a logarithmic function, $f(x_{ij}) = \ln x_{ij}$, with nodes distributed in a d -dimensional Euclidean space, \mathbb{R}^d , according to a Poisson point process with a constant density, δ .

A prominent real system following this rationale is the Internet at the autonomous systems (AS) level, where link directions represent customer-to-provider relationships between autonomous systems [28]. A link from AS i to AS j indicates the flow of money when Internet traffic is routed through that connection. Notice that, in general, ASs can act as customers in some connections and as providers in others. In this system, the term $\varepsilon_{out,i}$ represents the cost that AS i must pay to maintain a connection as a customer. Similarly, $\varepsilon_{in,j}$ represents the cost that AS j must pay to maintain a connection as a provider. These two costs generally depend on the size and physical infrastructure of each AS. Finally, the term $f(x_{ij})$ represents the cost associated with the physical constraints of the connection, such as, for instance, its physical length. In the case of very large ASs, a negative interaction energy, $\Delta\varepsilon_{ij}$, represents the synergistic effect of having a bidirectional connection, typically between the tier 1 ASs that define the core of the Internet.

In a different domain, brain connectomes are well described by the hyperbolic geometry network framework encoded by the directed \mathbb{S}^d model [16,29] and display an over-representation of reciprocal connections [30]. To form a synaptic connection, the costs of maintaining neurotransmitters and neuroreceptors are incurred, along with a cost associated with maintaining the neural fibers and the signal as it travels along the distance covered by them.

3.2.1. Non-Interacting Directed \mathbb{S}^d Model (NI-DSM)

When $\Delta\varepsilon_{ij} = 0$, the expected out-degree of a node with energy ε_{out} , located, without a loss of generality, at the origin of coordinates, is given by

$$\langle k_{out}(\varepsilon_{out}) \rangle = \delta \int \rho(\varepsilon_{in}) d\varepsilon_{in} \int_0^\infty \frac{V_{d-1} r^{d-1}}{1 + r^\beta e^{\beta(\varepsilon_{in} + \varepsilon_{out} - \mu)}} dr, \tag{29}$$

where $V_{d-1} = 2\pi^{d/2} / \Gamma(d/2)$ is the volume of a $(d - 1)$ -sphere. This expression can be rewritten for $\beta > d$ as

$$\langle k_{out}(\varepsilon_{out}) \rangle = \delta V_{d-1} I(\beta, d) \langle e^{-d\varepsilon_{in}} \rangle e^{d\mu} e^{-d\varepsilon_{out}}, \tag{30}$$

where

$$I(\beta, d) = \int_0^\infty \frac{t^{d-1} dt}{1 + t^\beta} = \frac{\pi}{\beta \sin \frac{d\pi}{\beta}}. \tag{31}$$

Thus, if we redefine the expected out- and in-degrees as $\kappa_{out} \equiv e^{-d\epsilon_{out}}$ and $\kappa_{in} \equiv e^{-d\epsilon_{in}}$, with $\mu = -\frac{1}{d} \ln(\delta V_{d-1} I(\beta, d) \langle k_{in} \rangle)$, the connection probability becomes

$$p_{ij} = \frac{1}{1 + \chi_{ij}^\beta} \text{ with } \chi_{ij} \equiv \frac{x_{ij}}{(\hat{\mu} \kappa_{out,i} \kappa_{in,j})^{\frac{1}{d}}}, \tag{32}$$

and

$$\hat{\mu} = \frac{\beta \Gamma\left(\frac{d}{2}\right) \sin\left(\frac{\pi d}{\beta}\right)}{2\delta \pi^{1+\frac{d}{2}} \langle k_{in} \rangle}. \tag{33}$$

(The case $\beta < d$ can be analyzed as in [18]). This model can be immediately identified as the directed variant of the \mathbb{S}^d model, first introduced in [16]. It represents a directed extension of the \mathbb{S}^d model originally proposed in [31], along with its equivalent formulation in the hyperbolic plane, known as the \mathbb{H}^2 model [32]. Notably, numerous analytical results have been derived for the $\mathbb{S}^1 / \mathbb{H}^2$ model, including studies on degree distribution [31–33], clustering [32–35], graph diameter [36–38], percolation [39,40], self-similarity [31], and spectral properties [41]. Moreover, this model has been extended to incorporate growing networks, weighted networks, multilayer networks, and networks with community structure, and it also serves as the foundation for defining a renormalization group for complex networks, see [26,27] and references therein. These analytical results and extensions of the undirected geometric model provide a guide for future studies of the Directed \mathbb{S}^d Model.

Unlike the DCM, geometry implies that the connection probability is size-independent. In turn, this implies that the reciprocity and clustering are finite, as shown in [16]. Interestingly, this model undergoes a topological phase transition at the critical inverse temperature $\beta_c = d$ [18]. For $\beta > \beta_c$, clustering is finite in the thermodynamic limit, whereas it vanishes below this value. This phase transition is of a topological nature and involves the reorganization of cycles in the network; transitioning from being short-range in the clustered phase to long-range in the unclustered one. This transition is accompanied by an anomalous behavior of the entropy per link. From Equation (4), we can compute the entropy as

$$\frac{S}{N \langle k_{in} \rangle} = \frac{2\beta}{d} \left(1 - \frac{\pi d}{\beta} \cot \frac{\pi d}{\beta} \right). \tag{34}$$

Unlike standard continuous phase transitions, the entropy per link diverges at the critical temperature from below as

$$\frac{S}{N \langle k_{in} \rangle} \sim \frac{1}{\beta - d}, \tag{35}$$

whereas it diverges logarithmically at higher temperatures. The origin of this anomalous behavior is due to the fact that the number of available microstates per link at low temperatures is finite, primarily connecting pairs of nodes at bounded distances. However, once the temperature surpasses the critical temperature, the number of available microstates becomes that of the order of the number of nodes, as links can now connect pairs of nodes that are arbitrarily far apart.

3.2.2. Interacting Directed \mathbb{S}^d Model (I-DSM)

When reciprocal links interact in the directed \mathbb{S}^d model, the strategy applied for the I-DCM, based on using Equation (13) to relate the connection probabilities in the interacting and non-interacting formulations, cannot be used because p_{ij}^{ni} is independent of the system size and does not approach zero in the thermodynamic limit. The probability of a directed link in the I-DSM must be found by substituting Equation (28) into Equation (7), with $\Delta\epsilon_{ij} \neq 0$, and imposing sparsity, which leads to new definitions of the chemical potential μ

and the relation between the expected in- and out-degrees of a given node and its in- and out-energies ϵ_{in} and ϵ_{out} . In particular, the connection probability can be written as

$$p_{ij} = \frac{\chi_{ji}^\beta + e^{-\beta\Delta\epsilon_{ij}}}{\chi_{ij}^\beta + \chi_{ji}^\beta + \chi_{ij}^\beta\chi_{ji}^\beta + e^{-\beta\Delta\epsilon_{ij}}}, \tag{36}$$

where

$$\chi_{ij} = x_{ij}e^{\epsilon_{out,i} + \epsilon_{in,j} - \mu}. \tag{37}$$

Using this expression, the average out-degree of a node with the in- and out-energies $\epsilon_{in,i}$ and $\epsilon_{out,i}$ can be written as

$$\begin{aligned} \langle k_{out}(\epsilon_{in,i}, \epsilon_{out,i}) \rangle &= \delta V_{d-1} e^{d\mu} e^{-d\epsilon_{out,i}} \times \\ &\times \int \int e^{-d\epsilon_{in,j}} \rho(\epsilon_{in,j}, \epsilon_{out,j}) d\epsilon_{in,j} d\epsilon_{out,j} \int_0^\infty \frac{t^{d-1} (q_{ij} t^\beta + e^{-\beta\Delta\epsilon_{ij}})}{t^\beta + q_{ij} (1 + t^\beta) t^\beta + e^{-\beta\Delta\epsilon_{ij}}} dt, \end{aligned} \tag{38}$$

where $q_{ij} \equiv e^{\epsilon_{out,j} - \epsilon_{out,i} + \epsilon_{in,i} - \epsilon_{in,j}}$. By integrating Equation (38) over the energies $\epsilon_{in,i}$ and $\epsilon_{out,i}$ and equating it to $\langle k_{in} \rangle$, we can obtain the value of the chemical potential μ from

$$e^{d\mu} = \frac{\langle k_{in} \rangle}{\delta V_{d-1} \langle e^{-d(\epsilon_{out,i} + \epsilon_{in,j})} \int_0^\infty \frac{t^{d-1} (q_{ij} t^\beta + e^{-\beta\Delta\epsilon_{ij}})}{t^\beta + q_{ij} (1 + t^\beta) t^\beta + e^{-\beta\Delta\epsilon_{ij}}} dt \rangle}, \tag{39}$$

where the average in the denominator is taken over the random variables $\epsilon_{in,i}, \epsilon_{in,j}, \epsilon_{out,i}, \epsilon_{out,j}$, and $\Delta\epsilon_{ij}$. Using a similar approach, the reciprocity becomes

$$r = \frac{\langle e^{-d(\epsilon_{out,i} + \epsilon_{in,j})} \int_0^\infty \frac{t^{d-1} e^{-\beta\Delta\epsilon_{ij}}}{t^\beta + q_{ij} (1 + t^\beta) t^\beta + e^{-\beta\Delta\epsilon_{ij}}} dt \rangle}{\langle e^{-d(\epsilon_{out,i} + \epsilon_{in,j})} \int_0^\infty \frac{t^{d-1} (q_{ij} t^\beta + e^{-\beta\Delta\epsilon_{ij}})}{t^\beta + q_{ij} (1 + t^\beta) t^\beta + e^{-\beta\Delta\epsilon_{ij}}} dt \rangle}. \tag{40}$$

Equation (38) implies that the average in- or out-degree of a given node depends on both ϵ_{in} and ϵ_{out} , not only on one of them, as is the case for non-interacting fermions. This indicates that computing the degree distributions requires the explicitly solving Equation (38). However, in the particular case of fully correlated ϵ_{in} and ϵ_{out} and $\Delta\epsilon_{ij} = \Delta\epsilon$, the term $q_{ij} = 1$, and the average in- or out-degree becomes a function of ϵ_{in} or ϵ_{out} separately. Thus, as in the case of non-interacting fermions, we can write $\kappa_{out} \equiv e^{-d\epsilon_{out}}$ and $\kappa_{in} \equiv e^{-d\epsilon_{in}}$, with

$$\mu = -\frac{1}{d} \ln(\delta V_{d-1} \tilde{I}(\beta, d, \Delta\epsilon) \langle k_{in} \rangle), \tag{41}$$

where

$$\tilde{I}(\beta, d, \Delta\epsilon) = \int_0^\infty \frac{t^{d-1} (t^\beta + e^{-\beta\Delta\epsilon})}{2t^\beta + t^{2\beta} + e^{-\beta\Delta\epsilon}} dt, \tag{42}$$

and the reciprocity becomes

$$r = \frac{\int_0^\infty \frac{t^{d-1} e^{-\beta\Delta\epsilon}}{2t^\beta + t^{2\beta} + e^{-\beta\Delta\epsilon}} dt}{\tilde{I}(\beta, d, \Delta\epsilon)}. \tag{43}$$

Figure 2 shows the results of the reciprocity in this case as a function of $\Delta\epsilon$ for different values of β . The reciprocity converges to one in the limit $\Delta\epsilon \rightarrow -\infty$ and approaches zero in the limit $\Delta\epsilon \rightarrow \infty$, as expected. Furthermore, it increases as the temperature rises. Note that the convergence to 1 with very low temperatures and/or a highly negative $\Delta\epsilon$ is only possible in the fully correlated case. In all other cases, the maximum possible value of the reciprocity is always less than one.

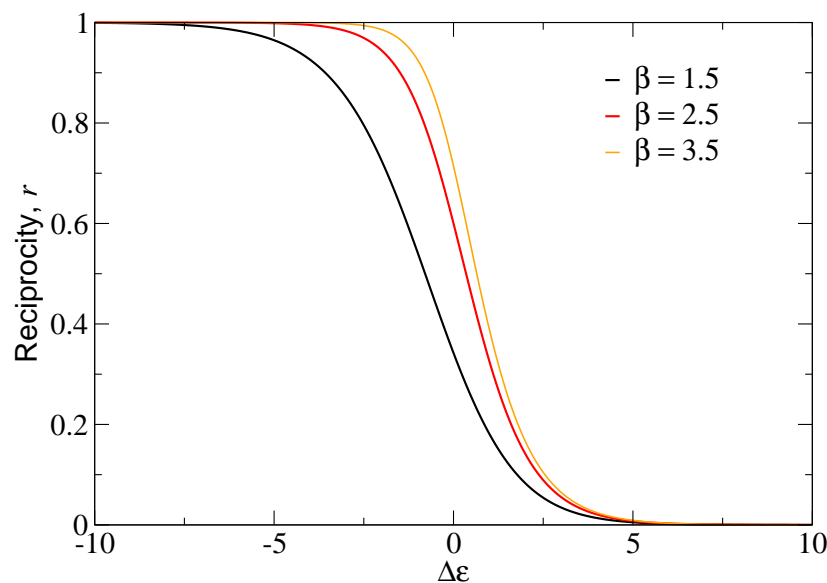


Figure 2. Reciprocity of the interacting directed \mathbb{S}^d model for fully correlated in- and out-energies, as a function of $\Delta\epsilon$. Different curves correspond to different temperatures β^{-1} .

4. Conclusions

The statistical mechanics framework for directed networks introduced in this work treats links as fermionic particles subject to constraints and interactions. This formalism allowed us to describe directed networks within a principled approach that incorporates the reciprocity and other structural properties, addressing the limitations of existing models. By leveraging concepts from quantum statistics, our methodology redefines network modeling, shifting the focus from node-centric descriptions to link interactions. Formulating directed networks within a grand canonical ensemble, we demonstrated how the chemical potential and key network features, such as the degree distribution and reciprocity, naturally emerge from the underlying statistical framework.

The versatility and analytical power of our formalism were illustrated through applications to specific cases, including the Directed Configuration Model and the Directed \mathbb{S}^d model. The key results highlighted the influence of interactions on the reciprocity and clustering. In the non-interacting formulations, the reciprocity vanishes in the thermodynamic limit, whereas in the interacting models, the framework supports a tunable reciprocity that remains finite under specific conditions. The inclusion of a geometric component in the \mathbb{S}^d model further showcased how spatial constraints shape the emergent properties of the network. This framework bridges theoretical advances with empirical applicability, providing a robust toolset for analyzing real-world directed networks. Additionally, it paves the way for exploring dynamical processes on directed topologies and designing models that better reflect the intricate balance of directed interactions. Future work could extend these principles to multilayer, temporal, or weighted networks, offering a deeper understanding of complex systems.

Author Contributions: M.B. and M.Á.S. both contributed equally to the conceptualization, methodology, formal analysis, investigation, writing—original draft preparation, writing—review and editing, and funding acquisition. All authors have read and agreed to the published version of the manuscript.

Funding: We acknowledge support from: Grant TED2021-129791B-I00 funded by MCIN/AEI/10.13039/501100011033 and by “European Union NextGenerationEU/PRTR”; Grant PID2022-137505NB-C22 funded by MCIN/AEI/10.13039/501100011033 and by “ERDF A way of making Europe”; and the

Generalitat de Catalunya grant number 2021SGR00856. M.B. acknowledges the ICREA Academia award, funded by the Generalitat de Catalunya.

Data Availability Statement: No new data were created.

Conflicts of Interest: The authors declare no conflicts of interest. The funders had no role in the design of the study; in the collection, analyses, or interpretation of data; in the writing of the manuscript; or in the decision to publish the results.

References

1. Newman, M.E.J. *Networks*; Oxford University Press: Oxford, UK, 2018.
2. Bianconi, G.; Gulbahce, N.; Motter, A.E. Local Structure of Directed Networks. *Phys. Rev. Lett.* **2008**, *100*, 118701. <https://doi.org/10.1103/PhysRevLett.100.118701>.
3. Asllani, M.; Lambiotte, R.; Carletti, T. Structure and dynamical behavior of non-normal networks. *Sci. Adv.* **2018**, *4*, eaau9403. <https://doi.org/10.1126/sciadv.aau9403>.
4. Boguñá, M.; Serrano, M.Á. Generalized percolation in random directed networks. *Phys. Rev. E* **2005**, *72*, 016106. <https://doi.org/10.1103/PhysRevE.72.016106>.
5. Serrano, M.Á.; De Los Rios, P. Interfaces and the edge percolation map of random directed networks. *Phys. Rev. E* **2007**, *76*, 056121.
6. Serrano, M.Á.; Boguñá, M.; Vespignani, A. Patterns of Dominant Flows in the World Trade Web. *J. Econ. Interact. Coord.* **2007**, *2*, 111–124.
7. Serrano, M.Á.; Klemm, K.; Vazquez, F.; Eguíluz, V.M.; San Miguel, M. Conservation laws for voter-like models on random directed networks. *J. Stat. Mech. Theory Exp.* **2009**, *2009*, P10024.
8. Asllani, M.; Challenger, J.D.; Pavone, F.S.; Sacconi, L.; Fanelli, D. The theory of pattern formation on directed networks. *Nat. Commun.* **2014**, *5*, 4517.
9. Muolo, R.; Carletti, T.; Gleeson, J.P.; Asllani, M. Synchronization dynamics in non-normal networks: The trade-off for optimality. *Entropy* **2020**, *23*, 36.
10. Nartallo-Kaluarachchi, R.; Asllani, M.; Deco, G.; Kringelbach, M.L.; Goriely, A.; Lambiotte, R. Broken detailed balance and entropy production in directed networks. *Phys. Rev. E* **2024**, *110*, 034313. <https://doi.org/10.1103/PhysRevE.110.034313>.
11. Park, J.; Newman, M.E.J. Statistical mechanics of networks. *Phys. Rev. E* **2004**, *70*, 066117. <https://doi.org/10.1103/PhysRevE.70.066117>.
12. Bianconi, G. Entropy of network ensembles. *Phys. Rev. E* **2009**, *79*, 036114. <https://doi.org/10.1103/PhysRevE.79.036114>.
13. Garlaschelli, D.; Loffredo, M.I. Patterns of link reciprocity in directed networks. *Phys. Rev. Lett.* **2004**, *93*, 268701. <https://doi.org/10.1103/PhysRevLett.93.268701>.
14. Fagiolo, G. Clustering in complex directed networks. *Phys. Rev. E—Stat. Nonlinear Soft Matter Phys.* **2007**, *76*, 026107.
15. Ahnert, S.E.; Fink, T.M.A. Clustering signatures classify directed networks. *Phys. Rev. E* **2008**, *78*, 036112. <https://doi.org/10.1103/PhysRevE.78.036112>.
16. Allard, A.; Serrano, M.Á.; Boguñá, M. Geometric description of clustering in directed networks. *Nat. Phys.* **2024**, *20*, 150–156.
17. Park, J.; Newman, M.E.J. Origin of degree correlations in the Internet and other networks. *Phys. Rev. E* **2003**, *68*, 026112. <https://doi.org/10.1103/PhysRevE.68.026112>.
18. Van der Kolk, J.; Serrano, M.Á.; Boguñá, M. An anomalous topological phase transition in spatial random graphs. *Commun. Phys.* **2022**, *5*, 245. <https://doi.org/10.1038/s42005-022-01023-w>.
19. Kim, H.; Del Genio, C.I.; Bassler, K.E.; Toroczkai, Z. Constructing and sampling directed graphs with given degree sequences. *New J. Phys.* **2012**, *14*, 023012.
20. Erdős, P.; Rényi, A. On random graphs I. *Publ. Math.* **1959**, *6*, 290–297.
21. Bianconi, G.; Barabási, A.L. Bose-Einstein Condensation in Complex Networks. *Phys. Rev. Lett.* **2001**, *86*, 5632–5635. <https://doi.org/10.1103/PhysRevLett.86.5632>.
22. Rushbrooke, G. On the statistical mechanics of assemblies whose energy-levels depend on the temperature. *Trans. Faraday Soc.* **1940**, *36*, 1055–1062.
23. Landsberg, P. Statistical Mechanics of Temperature-Dependent Energy Levels. *Phys. Rev.* **1954**, *95*, 643.
24. Elcock, E.; Landsberg, P. Temperature dependent energy levels in statistical mechanics. *Proc. Phys. Soc. Sect. B* **1957**, *70*, 161.
25. De Miguel, R.; Rubí, J.M. Statistical mechanics at strong coupling: A bridge between Landsberg’s energy levels and Hill’s nanothermodynamics. *Nanomaterials* **2020**, *10*, 2471.
26. Boguñá, M.; Bonamassa, I.; De Domenico, M.; Havlin, S.; Krioukov, D.; Serrano, M.Á. Network geometry. *Nat. Rev. Phys.* **2021**, *3*, 114–135. <https://doi.org/10.1038/s42254-020-00264-4>.

27. Serrano, M.Á.; Boguñá, M. *The Shortest Path to Network Geometry: A Practical Guide to Basic Models and Applications*; Cambridge University Press: Cambridge, UK, 2022. <https://doi.org/10.1017/9781108865791>.
28. Dimitropoulos, X.; Krioukov, D.; Fomenkov, M.; Huffaker, B.; Hyun, Y.; Claffy, K.; Riley, G. AS relationships: Inference and validation. *ACM SIGCOMM Comput. Commun. Rev.* **2007**, *37*, 29–40.
29. Allard, A.; Serrano, M.Á. Navigable maps of structural brain networks across species. *PLOS Comput. Biol.* **2020**, *16*, e1007584.
30. Lin, A.; Yang, R.; Dorkenwald, S.; Matsliah, A.; Sterling, A.R.; Schlegel, P.; Yu, S.c.; McKellar, C.E.; Costa, M.; Eichler, K.; et al. Network statistics of the whole-brain connectome of *Drosophila*. *Nature* **2024**, *634*, 153–165.
31. Serrano, M.Á.; Krioukov, D.; Boguñá, M. Self-Similarity of Complex Networks and Hidden Metric Spaces. *Phys. Rev. Lett.* **2008**, *100*, 078701. <https://doi.org/10.1103/PhysRevLett.100.078701>.
32. Krioukov, D.; Papadopoulos, F.; Kitsak, M.; Vahdat, A.; Boguñá, M. Hyperbolic geometry of complex networks. *Phys. Rev. E* **2010**, *82*, 036106. <https://doi.org/10.1103/PhysRevE.82.036106>.
33. Gugelmann, L.; Panagiotou, K.; Peter, U. Random Hyperbolic Graphs: Degree Sequence and Clustering. In Proceedings of the Automata, Languages, and Programming, ICALP 2012, Part II, Warwick, UK, 9–13 July 2012; Czumaj, A., Mehlhorn, K., Pitts, A., Wattenhofer, R., Eds.; Lecture Notes in Computer Science; Springer: Berlin/Heidelberg, Germany, 2012; Volume 7392, pp. 573–585. https://doi.org/10.1007/978-3-642-31585-5_51.
34. Candellero, E.; Fountoulakis, N. Clustering and the Hyperbolic Geometry of Complex Networks. *Internet Math.* **2016**, *12*, 2–53. <https://doi.org/10.1080/15427951.2015.1067848>.
35. Fountoulakis, N.; van der Hoorn, P.; Müller, T.; Schepers, M. Clustering in a hyperbolic model of complex networks. *Electron. J. Probab.* **2021**, *26*, 1–132. <https://doi.org/10.1214/21-EJP583>.
36. Abdullah, M.A.; Fountoulakis, N.; Bode, M. Typical distances in a geometric model for complex networks. *Internet Math.* **2017**, *1*, 115–126. <https://doi.org/10.24166/im.13.2017>.
37. Friedrich, T.; Krohmer, A. On the Diameter of Hyperbolic Random Graphs. *SIAM J. Discret. Math.* **2018**, *32*, 1314–1334. <https://doi.org/10.1137/17M1123961>.
38. Müller, T.; Staps, M. The diameter of KPKVB random graphs. *Adv. Appl. Probab.* **2019**, *51*, 358–377. <https://doi.org/10.1017/apr.2019.23>.
39. Serrano, M.Á.; Krioukov, D.; Boguñá, M. Percolation in Self-Similar Networks. *Phys. Rev. Lett.* **2011**, *106*, 048701. <https://doi.org/10.1103/PhysRevLett.106.048701>.
40. Fountoulakis, N.; Müller, T. Law of large numbers for the largest component in a hyperbolic model of complex networks. *Ann. Appl. Probab.* **2018**, *28*, 607–650. <https://doi.org/10.1214/17-AAP1314>.
41. Kiwi, M.; Mitsche, D. Spectral gap of random hyperbolic graphs and related parameters. *Ann. Appl. Probab.* **2018**, *28*, 941–989. <https://doi.org/10.1214/17-AAP1323>.

Disclaimer/Publisher’s Note: The statements, opinions and data contained in all publications are solely those of the individual author(s) and contributor(s) and not of MDPI and/or the editor(s). MDPI and/or the editor(s) disclaim responsibility for any injury to people or property resulting from any ideas, methods, instructions or products referred to in the content.